THE JOURNAL OF PHYSICAL CHEMISTRY B

 VOLUME 106, NUMBER 2, JANUARY 17, 2002

LETTERS

Imaging and Manipulation of Gold Nanorods with an Atomic Force Microscope

Shuchen Hsieh, Sheffer Meltzer, C. R. Chris Wang,† Aristides A. G. Requicha, Mark E. Thompson, and Bruce E. Koel*

Laboratory for Molecular Robotics, University of Southern California, Los Angeles, California 90089-0482, and Department of Chemistry, National Chung Cheng University, Min-Hsiung, Chia-Yi 621, Taiwan, Republic of China

Received: July 17, 2001; In Final Form: October 18, 2001

Designed fabrication of nanostructures requires progress on a number of fronts in research and development. The ability to synthesize, deposit, and position nanometer scale materials is important for the development of this technology. We report here on studies of deposition and manipulation of electrochemically prepared, micelle-capped Au nanorods deposited on silicon dioxide (SiO_2) surfaces. A thiol-terminated silane (3-mercaptopropylmethyldimethoxysilane, MPMDMS) was used as an active interface for gold nanorod assembly. A scanning force microscope (SFM) was used to image and manipulate individual Au nanorods. It was found that mechanical movement of the rods depends on the location of the pushing point along the rod.

Introduction

Fabrication of nanostructures using different materials and methods is a rapidly growing field of interdisciplinary research.[1−3] Advances in fabricating nanoscale devices will occur with improvements in the ability to synthesize, deposit, and position *nano*-building blocks on suitably designed substrates. Several techniques employing different strategies have been used to create patterned nanostructures on surfaces. Recent methods include the use of existing surface structures as a template, local deposition of material from a scanning probe microscope (SPM) tip, and direct manipulation of deposited nanoclusters using an SPM tip.

One effective approach is to use chemical templates or inherent surface structural templates, e.g., atomic steps, reconstruction sites, and grain boundaries, for patterning nanostructures by subsequent deposition of the desired material. For example, Smalley and co-workers[4] demonstrated deposition of single-walled nanotube segments on chemically functionalized, nanolithographic templates, Batzill et al.[5] grew Ag nanowires by Ag deposition on a stepped surface of a CaF_2 single crystal, and Penner and co-workers[6] demonstrated electrodeposition of molybdenum at step edges on graphite. Physical effects have also been used to align nanowires and nanotubes during the deposition process. An electric field was used by Smith et al.[7] to align metallic nanowires, and Lieber and co-workers[8] showed the assembly of semiconductor nanowire arrays by combining fluidic alignment with surface-patterning techniques.

The high-resolution capability of SPM techniques has also been used for the fabrication of nanostructures. Nanopattern formation by local deposition of metal clusters using a scanning tunneling microscope (STM) tip has been demonstrated by several groups. Kolb et al.[9,10] mechanically deposited Cu clusters on Au in an electrochemical environment. Similar results were demonstrated using electrodeposition to deposit Ag clusters onto a Au(111) surface,[11] and magnetic Co clusters were deposited from an aqueous electrolyte onto a Au surface by Hofman et

* Corresponding author. Tel: +1-213-740-4126. Fax: +1-213-740-3972. E-mail: koel@chem1.usc.edu.
† National Chung Cheng University.

10.1021/jp012747x CCC: $22.00
Published on Web 12/18/2001

al.[12] Also, an STM tip has been used to initiate linear chain polymerization of an adsorbed layer of monomolecular moieties.[13]

A third approach, and the one used in this study, is to deposit pre-synthesized metal clusters on a substrate and position them in a desired pattern using a scanning force microscope (SFM) tip. Since it is now possible to synthesize multicomponent metal nanoparticles using a combination of templates and layer-by-layer self-assembly, this *bottom-up* positioning approach is well suited for creating large structures from novel, precisely made building blocks.[14] In our laboratory, we have demonstrated controlled manipulation by mechanical "pushing", using an atomic force microscope (AFM) tip, of individual[18,19] and linked[20] gold particles, and use of gold particles as templates for subsequent deposition processes.[21] More recently, the positioning of individual carbon nanotubes on a SiO_2 substrate by mechanical pushing was demonstrated.[15] This setup was also used to study the nanomechanical[16] and electrical properties of the carbon nanotubes.[17]

One possible extension of such nanomanipulation work is to use nanorods as fundamental building blocks to create novel structures. The shape and size of metallic nanorods make them excellent models to study the electrical and optical[22] properties of nanowires, as well as frictional forces and nanometer-scale mechanics. Several groups have demonstrated the ability to synthesize colloidal nanorods with well-defined sizes and shapes using different materials.[23,24] In particular, gold nanorods have been prepared by electrochemical methods.[25,26] These procedures have produced gold nanorods with mean aspect ratios ranging from 1 to greater than 10. Most of these studies have used TEM and other spectroscopic techniques to analyze the size and shape distributions of the synthesized rods. To the best of our knowledge, AFM has not been used yet as a complementary characterization technique.

Despite the wide range of research that has dealt with synthesis issues, very little research has been devoted to the self-assembly and alignment of rod-shaped nanocrystals. One of the few examples available is from El-Sayed's lab where a variety of ordered structures could be formed under controlled experimental conditions.[27]

In this study, we have deposited gold nanorods on a MPMDMS (3-mercaptopropylmethyldimethoxysilane)-modified SiO_2/Si (111) substrate, imaged the rods using dynamic mode AFM, and subsequently performed manipulation using the AFM tip. The objective of this work was to demonstrate that these gold nanorods can be utilized as functional "primatives" or building blocks for nanostructure fabrication.

Experimental Section

A Si (111) wafer (P/B, International Wafer Service) was cut into 1×1 cm^2 pieces and cleaned by immersing the Si wafer in a "piranha" bath (30% H_2O_2 mixed in a 1:4 ratio with concentrated H_2SO_4) at 100 °C for 10 min, and then rinsing with ethanol (Aldrich, spectrophotometric grade). The sample was then stored in ethanol for later use. Deposition of 3-mercaptopropylmethyldimethoxysilane (MPMDMS, Gelest Inc. PA) was achieved by immersing the substrate into a 1:20 (volume ratio) solution of MPMDMS in ethanol for 12 h. Subsequently, the samples were rinsed with ethanol and then dried in a stream of pure nitrogen.

The electrochemical method for synthesis of suspended Au nanorods has been described previously.[28] The gold nanorods are capped with hexadecyltrimethylammonium bromide (C_{16}TAB) and suspended in an aqueous solution. Excess surfactant was removed using a centrifugation procedure (Clay Adams Dynac Centrifuge; 3300 rpm at 25 °C for 20 min). A droplet of the gold nanorod solution was placed onto the MPMDMS-modified silicon substrate and allowed to dry in air. Once dry, the sample was carefully rinsed with DI water and then dried again under nitrogen.

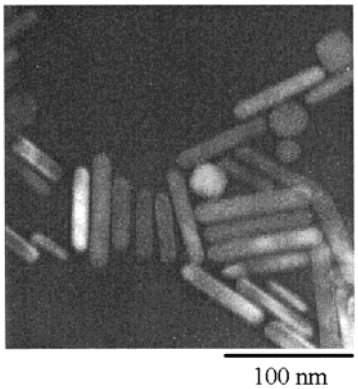

Figure 1. TEM images of gold nanorods that were synthesized electrochemically and have an aspect ratio of 4 to 9.

X-ray photoelectron spectroscopy (XPS) data was obtained using a Physical Electronics Model 5300 ESCA spectrometer equipped with an Al Kα (1486.6 eV) X-ray source and using a pass energy of 90 eV. Transmission electron microscopy (TEM) (Philips 420; 120 keV) was used to analyze the nanorod size and shape distributions.

AFM imaging and manipulation experiments were carried out using an Autoprobe CP AFM (Park Scientific Instruments) operated in dynamic mode in air, using triangularly shaped silicon cantilevers (Park Scientific Instruments, 13.0 N m^{-1} spring constant, and 340 kHz resonance frequency). The setup that was used for AFM nanomanipulation has been described previously.[29,30] It is based on Probe Control Software (PCS) developed in our group and built upon the application programming interface (API) provided by PSI.

Results and Discussion

Gold nanorods were prepared by an electrochemical method in which a gold electrode is used as the sacrificial anode and a platinum electrode is used as the cathode. Both electrodes were immersed in an electrolyte solution consisting of cationic surfactant, C_{16}TAB, which serves both as the supporting electrolyte and stabilizer to prevent agglomeration of the formed rods. Figure 1 shows a TEM image of the synthesized nanorods. The nanorod dimensions were measured to be 10 ± 2 nm in diameter and 70 ± 20 nm in length, with a shape distribution that was typical for the image shown.

It is well-known that colloidal gold particles with ionic shells can be deposited on surfaces that have been modified by layers having end groups with high affinity for gold (i.e., CN, SH, NH_2).[31] Electrostatic and/or chemical interactions between the gold and these groups bind the particles to the substrate. Amine-terminated adhesive layers are commonly used for this purpose; however, we found that such layers were not useful for these particular studies. We believe that this is because the micelle (C_{16}TAB) used to stabilize the gold nanorods in aqueous solution is positively charged overall.[25] A tentative model has been proposed to describe the surfactant behavior at the gold surface, in which the surfactant cations are oriented toward the gold in the inner shell, while in the second layer (outer shell), the polar group faces toward the water solution. Therefore, adsorption on a positively charged adhesive layer is electrostatically

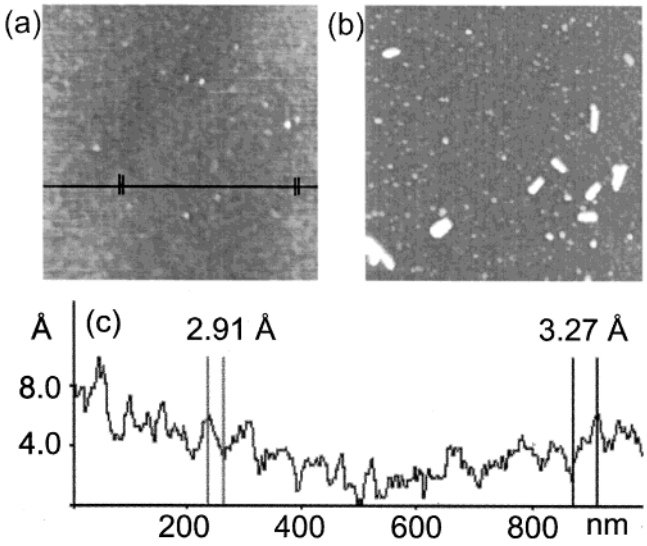

Figure 2. AFM images (1μm × 1μm) of MPMDMS-modified SiO_2/Si substrate (a) before and (b) after gold-nanorod deposition. As shown in (c), the MPMDMS layer is nearly featureless with a RMS roughness of 2 Å. The height scale from black to white is 2 nm in (a) and 10 nm in (b).

SCHEME 1

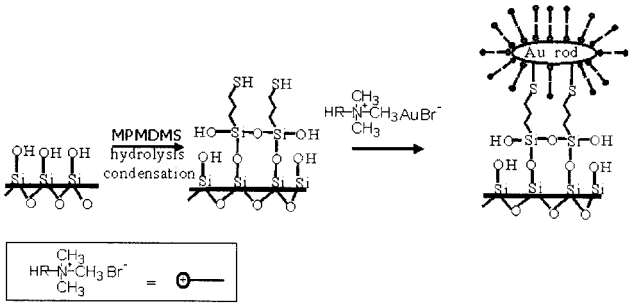

hindered. To check this model, we tried to deposit the rods on an amine-terminated substrate. No evidence for deposition of gold nanorods was observed by using XPS or AFM (results not shown). However, we found that a thiol-terminated adhesive layer could be used successfully for rod deposition and assembly. A schematic representation of the sample deposition process is illustrated in Scheme 1. In "open" or ambiant atmosphere conditions, we found that the di-methoxy silane compound forms a very smooth monolayer while the tri-methoxy compound formed a rough layer with 1−2 nm agglomerate features. These poly-siloxane agglomerates result from homogeneous polymerization in solution and deposit on the substrate. The di-methoxy compound was found also to be less sensitive to humidity and small amounts of water in the organic solvent. This may be because there is one less "oxy" site available for condensation between silane molecules in solution and therefore less homogeneous polymerization takes place.

Figure 2a shows an AFM image (1 μm × 1 μm) of a 3-MPMDMS-modified silicon substrate. Figure 2c shows a cross section analysis of this image. It is evident in these figures that the self-assembled monolayer that is formed is smooth and does not contain any silane agglomerates. The overall RMS value of the scanned area was calculated to be 2 Å.

The AFM image in Figure 2b shows the surface after gold nanorod deposition on this substrate. The nanorod heights measured by AFM of 10 ± 2 nm correspond well to the diameter

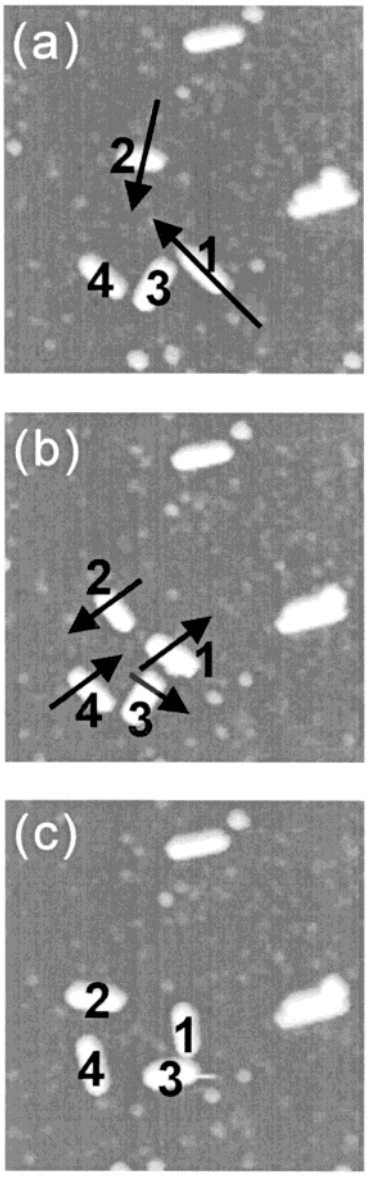

Figure 3. A sequence of SFM images (500 nm × 500 nm scan size) displaying the manipulation of four gold nanorods. The arrows in each image show the manipulation direction that results in the rod configuration in the next image. (a) Initial arrangement of the rods; (b) result of translational manipulations of "1" along its longitudinal axis and "2" across this axis; (c) results of rotational manipulation operations of all 4 rods by ±45° relative to their original orientation. The height scale from black to white is 10 nm for (a−c).

observed in TEM. The apparent shape and length of the nanorods observed by AFM differ from those observed in TEM because of well-known tip-convolution effects in the XY plane.

XPS was used to confirm the presence of gold on the substrate after this procedure for depositing the nanorods. The presence of characteristic Au 4d and 4f peaks proves that there is gold on the surface. On the basis of the AFM images in Figure 2 and the XPS data, we conclude that gold nanorods were indeed deposited on the 3-MPMDMS-modified silicon substrate.

Results from a nanorod manipulation experiment are shown in Figure 3. First, we located an area on the substrate with several nanorods in close proximity. An AFM image (500 nm × 500 nm scan size) of this area is shown in Figure 3a. Four nanorods, marked as "1" to "4", were manipulated in different orientations to study the effects of the precise location of the

pushing point on the resulting position of the manipulated rod. The arrows in Figure 3 indicate the manipulation direction that produced the arrangement shown in the following image. Figure 3b shows the results of single pushing operations on rods "1" and "2". When the nanorod labeled as "1" was pushed along its longitudinal axis, this resulted in a perfect translation of the nanorod in the manipulation direction. When we pushed the rod labeled as "2" in a direction perpendicular to this axis by contact with the rod at its center the result was a translation with a small rotation. Figure 3c shows fine control in rotational manipulation operations (indicated by the arrows in Figure 3b) of all 4 rods by ±45° relative to their original orientations. These rotation manipulations were achieved by pushing on the nanorods at "off-center" locations, near the ends, in a direction perpendicular to the longitudinal axis. This overall set of manipulation operations formed a square-like arrangement of four nanorods.

Translational manipulation of a nanorod without rotation takes place whenever the tip hits the nanorod at its center. In these experiments, we found that it was easier to translate the rods when the pushing direction was along the longitudinal axis than when pushing was done transverse to this axis. This is because it is easy to locate the highest point across the width of the rod (which is the center of the rod) than to determine precisely the center of the rod along the long axis of the rod. Therefore, the result of longitudinal manipulation was often perfect translation while transverse manipulation often caused a combination of translation and rotation. This information on rod manipulation is important for applications that use the rods to accurately assemble a functional nanostructure. It will be somewhat complicated to build such structures with nanorods, because after the rods are roughly positioned, subsequent movements may have to specify both position and angle of the nanorods.

By tracking the tip amplitude and deflection signals during the manipulation operation it is possible to estimate the mechanical threshold needed for manipulation.[17] These signals can also be used to compare interactions between different particles and adhesive layers. Further detailed studies comparing manipulation of nanorods and nanoparticles are in progress.

Conclusions

We report results demonstrating AFM imaging and controlled manipulation of gold nanorods on an MPMDMS-modified SiO_2/Si(111) substrate. Nanorod deposition from solution was characterized by using AFM and XPS. Using PCS software, translational and rotational manipulation of the rods by AFM was demonstrated, showing that a high degree of positional control could be achieved. It was found that manipulation of the rods depends on the exact position of the pushing point along the rod. This work demonstrates that Au nanorods can be used as building blocks to form nanostructures in much the same way as nanoparticles have been used in the past. Such nanorods should be useful as elements in a variety of functional nanostructures and fundamental studies of nanometer-scale friction and manipulation.

Acknowledgment. We thank Dr. Michael Quinlan for taking the XPS spectra and for helpful discussions, and David Beck for useful comments. This research was supported by the NSF under Grant EIA-98-71775.

References and Notes

(1) Xia, Y.; Rogers, J. A.; Paul, K. E.; Whitesides, G. M. *Chem. Rev.* **1999**, *99*, 1823−1848.
(2) Nyffenegger, R. M.; Penner, R. M. *Chem. Rev.* **1997**, *97*, 1195.
(3) McCarty, G. S.; Weiss, P. S. *Chem. Rev.* **1999**, *99*, 1983−1990.
(4) Jie, L.; Casavant, M. J.; Cox, M.; Walters, D. A.; Boul, P.; Wei, L.; Rimberg, A. J.; Smith, K. A.; Colbert, D. T.; Smalley, R. E. *Chem. Phys. Lett.* **1999**, *303*, 125−129.
(5) Batzill, M.; Sarstedt, M.; Snowdon, K. J. *Nanotechnology* **1998**, *9*, 20−29.
(6) Zach, M. P.; Ng, K. H.; Penner, R. M. *Science* **2000**, *290*, 2120.
(7) Smith, P. A.; Nordquist, C. D.; Jackson, T. N.; Mayer, T. S.; Martin, B. R.; Mbindyo, J.; Mallouk, T. E. *Appl. Phys. Lett.* **2000**, *77*, 1399−1401.
(8) Yu, H.; Xiangfeng, D.; Qingqiao, W.; Lieber, C. M. *Science* **2001**, *291*, 630−633.
(9) Kolb, D. M.; Ullmann, R.; Will, T. *Science* **1997**, *275*, 1097−1099.
(10) Ullmann, R.; Will, T.; Kolb, D. M. *Chem. Phys. Lett.* **1993**, *209*, 238.
(11) Zamborini, F. P.; Crooks, R. M. *J. Am. Chem. Soc.* **1998**, *120*, 9700−9701.
(12) Hofman, D.; Schindler, W.; Kirschner, J. *Appl. Phys. Lett.* **1998**, *73*, 3279−3281.
(13) Okawa, Y.; Aono, M. *Nature* **2001**, *409*, 683−684.
(14) Kovtyukhova, N. I.; Martin, B. R.; Mbindyo, J. K. N.; Mallouk, T. E.; Cabassi, M.; Mayer, T. S. *Mater. Sci. Eng., B*, submitted.
(15) Avouris, P.; Hertel, T.; Martel, R.; Schmidt, T.; Shea, H. R.; Walkup, R. E. *Appl. Surf. Sci.* **1999**, *141*, 201.
(16) Falvo, M. R.; Taylor, R. M., II; Helser, A.; Chi, V.; Brooks, F. P., Jr.; Washburn, S.; Superfine, R. *Nature* **1999**, *397*, 236−238.
(17) Postma, H. W. C.; de Jonge, M.; Dekker, C. *Phys. Rev. B* **2000**, *62*, R10653−R10656.
(18) Baur, C.; Bugacov, A.; Koel, B. E.; Madhukar, A.; Montoya, N.; Ramachandran, T. R.; Requicha, A. A. G.; Resch, R.; Will, P. *Nanotechnology* **1998**, *9*, 360−364.
(19) Resch, R.; Baur, C.; Bugacov, A.; Koel, B. E.; Madhukar, A.; Requicha, A. A. G.; Will, P. *Langmuir* **1998**, *14*, 6613−6616.
(20) Resch, R.; Baur, C.; Bugacov, A.; Koel, B. E.; Echternach, P. M.; Madhukar, A.; Montoya, N.; Requicha, A. A. G.; Peter, W. *J. Phys. Chem. B* **1999**, *103*, 3647−3650.
(21) Meltzer, S.; Resch, R.; Koel, B. E.; Thompson, M. E.; Madhukar, A.; Requicha, A. A. G.; Will, P. *Langmuir* **2001**, *17*, 1713−1718.
(22) Mohamed, M. B.; Volkov, V.; Link, S.; El-Sayed, M. A. *Chem. Phys. Lett.* **2000**, *317*, 517−523.
(23) Link, S.; El-Sayed, M. A. *J. Phys. Chem. B* **1999**, *103*, 8410−8426.
(24) Martin, B. R.; Dermody, D. J.; Reiss, B. D.; Fang, M.; Lyon, L. A.; Natan, M. J.; Mallouk, T. E. *Adv. Mater.* **1999**, *11*, 1021−1025.
(25) Ser-Sing, C.; Chao-Wen, S.; Cheng-Dah, C.; Wei-Cheng, L.; Wang, C. R. C. *Langmuir* **1999**, *15*, 701−709.
(26) El-Sayed, M. *Acc. Chem. Res.* **2001**, *34*, 257−264.
(27) Nikoobakht, B.; Wang, Z. L.; El-Sayed, M. A. *J. Phys. Chem. B* **2000**, *104*, 8635−8640.
(28) Yu-Ying, Y.; Ser-Sing, C.; Chien-Liang, L.; Wang, C. R. C. *J. Phys. Chem. B* **1997**, *101*, 6661−6664.
(29) Baur, C.; Gazen, B. C.; Koel, B.; Ramachandran, T. R.; Requicha, A. A. G.; Zini, L. *J. Vac. Sci. Technol. B* **1996**, *15*, 1577−80.
(30) Resch, R.; Bugacov, A.; Baur, C.; Koel, B. E.; Madhukar, A.; Requicha, A. A. G.; Will, P. *Appl. Phys. A* **1998**, *A67*, 265−271.
(31) Grabar, K. C.; Griffith Freeman, R.; Hommer, M. B.; Natan, M. *J. Anal. Chem.* **1995**, *67*, 735.